ELSEVIER

Journal of Nuclear Materials 283–287 (2000) 198–204

journal of nuclear materials

www.elsevier.nl/locate/jnucmat

Effects of grain boundary misorientation on solute segregation in thermally sensitized and proton-irradiated 304 stainless steel

T.S. Duh, J.J. Kai *, F.R. Chen

Department of Engineering and System Science, Center of Electron Microscopy, National Tsing Hua University, 101 Section II, Kuang-fu Road, Hsin-chu, 300 Taiwan, ROC

Abstract

The purpose of this study is to investigate the effects of the grain boundary misorientation on the radiation-induced segregation (RIS) in 304 stainless steels. There were four test conditions for the specimens: (1) as-received (AR) with enriched Cr at grain boundary, (2) AR + 1 dpa proton irradiation at 450°C, (3) thermally sensitized (SEN), and (4) SEN + 1 dpa proton irradiation at 450°C. The Cr/Ni-concentration profiles were measured by using FEGTEM/EDS and the grain boundary misorientation was determined with the aid of simulated Kikuchi patterns. A delayed Cr depletion compared to no pre-enrichment condition was found at grain boundaries in AR + 1 dpa specimens. The Cr-concentration profile gets narrower and deeper in SEN + 1 dpa specimens. The degree of grain boundary segregation was observed to be higher at random boundaries than special boundaries. The segregation cusps were measured at grain boundaries of $\Sigma 3$, $\Sigma 9$ and $\Sigma 15$ in SEN + 1 dpa 304 stainless steel specimens. From the fitted segregation cusps, it seems that the Cr segregation level at special boundaries in irradiated sensitized 304 stainless steels increases with Σ for values up to $\Sigma = 15$.

1. Introduction

Many studies have indicated that some of the grain boundary related properties, such as grain boundary energy [1], grain boundary migration [2], grain boundary diffusion [3], and grain boundary segregation are dependent upon the grain boundary structure. For grain boundary segregation [4], small angle boundaries generally exhibit smaller amounts of segregation than large angle boundaries. The increase in the degree of segregation with misorientation can be attributed to the increase in primary dislocation density with misorientation. For large angle boundaries, the variations in segregation to most grain boundaries maybe up to $\pm 30\%$ of the average in polycrystalline specimens [5]. In general, the high-energy grain boundaries have more preferential sites for solute segregation than the low-energy boundaries such as CSL (Coincidence Site Lattice) grain boundaries, especially $\Sigma 3$ twin boundaries.

The CSL model along with the dislocation model is a convenient way to describe the structure of high-angle boundaries in materials with cubic crystal symmetry. The parameter, Σ, in the CSL model is the reciprocal density of coincidence sites. Normally, boundaries in general polycrystalline specimens are not exact CSL boundaries, rather a deviation from the CSL boundaries. Therefore, it is customary to divide boundaries into 'special' boundaries and 'general' boundaries according to the Brandon's criterion [6].

The effects of grain boundary structure on grain boundary segregation have been studied by many workers [4,7,8] in past years. However, the effect of grain boundary structure on radiation-induced segregation (RIS) has not been investigated. In this study, we were interested in the effect of grain boundary misorientation on RIS in proton irradiated 304SS. It is well known that Cr depletion near grain boundaries is a major factor causing IASCC [9] and IGSCC in irradiated and thermally sensitized (SEN) austenitic stainless steels, respectively. The mechanisms of these two grain boundary segregation phenomena are different. The thermal sensitization effect is driven by the thermodynamic forces. In contrast, RIS is a non-equilibrium effect and is driven

* Corresponding author. Tel.: +886-3 5715131; fax: +886-5720724.

E-mail address: jjkai@faculty.nthu.edu.tw (J.J. Kai).

0022-3115/00/$ - see front matter
PII: S0022-3115(00)00255-5

by kinetic processes [10]. The Cr depletion during thermal sensitization is caused by the diffusion of Cr and carbon to grain boundaries and formation of Cr carbides at the grain boundaries. The mechanism of RIS can be described by the inverse Kirkendall model.

2. Experimental

The 304SS used in this work had the following composition (in wt%): Cr(18.04), Ni(8.23), Mn(1.49), Mo(0.036), P(0.025), S(0.002), Si(0.5), N(0.056), C(0.047) and Fe(bal.). There were two initial conditions, as-received and sensitized, for the irradiated specimens; therefore we had four different conditions for the specimens: as-received (AR), irradiated, sensitized (SEN) and sensitized-irradiated. The heat treatment for sensitization was carried out at 650°C for 100 h and then cooled by water quench. The heat treatment for the AR specimen was at 1100°C for 3 min and cooled by water quench. The irradiation tests were performed using a Tandem inear accelerator to promote the RIS effect in both the AR and SEN 304SS specimens. The specimens were irradiated by 5 MeV protons at 450°C to a total dose of 1 dpa. The damage rate was estimated at about 1×10^{-6} dpas/s at the examined region. After irradiation, both the SEN and AR samples were made into transmission electron microscopy (TEM) specimens 3 mm in diameter and 80–90 μm thick and then prepared by electropolishing for TEM observations.

The observations of grain boundary segregation and grain boundary misorientation were performed on JEOL JEM-2010F TEM with an X-ray spectrometer attached to the stage. This instrument provides an acceleration voltage of 200 kV and has a small beam size of 0.5 nm. The Cr/Ni-concentration profiles near the grain boundary were measured by X-ray energy dispersive spectrometry (XEDS) and the grain boundary misorientations were determined by diffraction patterns with Kikuchi maps. The specimens were sputtered with Ar ions to clean the surface before EDS measurement. The X-ray spectra profiles across grain boundaries were taken normally at ± 0, 2, 4, 10, 20, 50, 70 nm steps, and the spectra were taken along the grain boundaries for a minimum of five measurements (>5 nm apart) on each edge-on grain boundary. Each X-ray spectrum was collected for 90 s with the beam probe checked and repositioned every 30 s to keep the drift less than 1–2 nm.

3. Results

3.1. Grain boundary segregation

The representative concentration profiles across grain boundaries are shown in Fig. 1 for both the AR and irradiated 304SS specimens. From Fig. 1, the Cr enrichment and Fe depletion can be found near grain boundaries in the AR specimens. The Cr-enrichment levels at grain boundaries are different from boundary to boundary and are listed in Table 1. The majority of the enriched Cr and depleted Fe atoms at general grain boundaries typically lie in a narrow zone of 3–4 nm. However, for the Σ3 boundary the concentration profiles of Cr, Fe and Ni are almost flat curves across the grain boundaries, and this could be attributed to the fact that the Σ3 boundaries generally have a more ordered close-packed structure than the general boundaries. For the irradiated case, we see from Table 1 that most of the data, compared with those of RIS and sensitization, indicate no obvious changes in concentrations of Cr and Ni atoms near the grain boundaries after 1 dpa irradiation, and this can also be seen in Fig. 1 (solid lines) which shows the flat concentration profiles of Fe, Cr and Ni atoms near the grain boundary in irradiated specimens. The average concentration of chromium at general grain boundaries (not including Σ3 boundaries) in irradiated 304SS specimens is about 19.6 at.%, only 0.7% lower than that of matrix, and for Nickel, the average concentration at general boundaries is about 8.3 at.%, which is 1% higher than that of matrix. From the above experimental results, we can see that the degree of RIS to grain boundaries is normally small for the 1-dpa irradiated 304SS specimens with initially enriched Cr at grain boundaries.

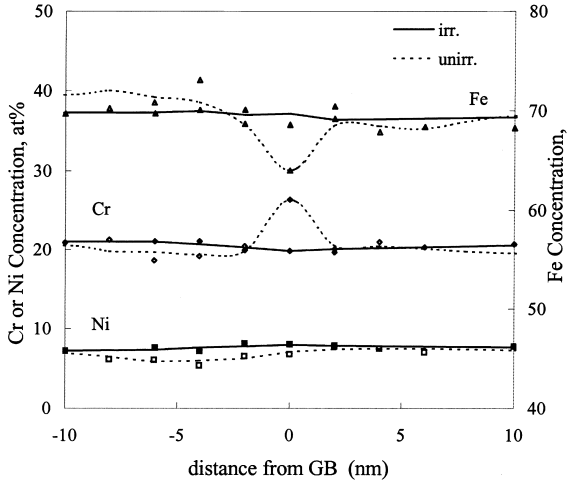

Fig. 1. Concentration profiles near grain boundaries in AR (dashed lines) and AR + 1 dpa (solid lines) specimens.

The representative concentration profiles across grain boundaries are shown in Fig. 2 for both the sensitized and irradiated-sensitized 304SS specimens. For sensitized specimens, depletion of Cr and enrichment of Fe and Ni at grain boundaries of different misorientations were generally observed. The segregation level of Cr and

Table 1
Grain boundary misorientation relationships for AR and AR + 1 dpa 304SS specimens

Boundary No.	Nearest Σ	Misorientation angle/axis	$\Delta\theta <$ Bran. cri.[a]	ΔCr at.%	ΔNi at.%
AR304					
1	3	59.7°/0.6, 0.6, 0.6	0.7 < 8.7°	0.7	0.0
2	3	59.8°/0.6, 0.6, 0.6	1.6 < 8.7°	1.2	0.3
3	11	48.1°/0.8, 0.6, 0.0		3.2	−0.2
4	15	44.0°/0.8, 0.6, 0.1		1.2	−0.7
5	15	45.2°/0.9, 0.5, 0.0	3.7 < 3.9°	3.0	−1.1
6	21b	45.3°/0.7, 0.5, 0.4		3.0	−0.5
7	35a	27.8°/0.8, 0.5, 0.4		3.5	−0.5
8	43b	23.1°/0.8, 0.5, 0.0		2.5	0.4
9	*	29.8°/0.7, 0.6, 0.3		4.7	−0.4
10	*	27.8°/0.8, 0.5, 0.4		6.5	−0.7
11	*	36.5°/1.0, 0.3, 0.1		5.6	−0.5
AR304 + 1 dpa at 450°C					
12	3	59.8°/0.6, 0.6, 0.6	0.8 < 8.7°	−0.8	2.1
13	9	37.9°/0.7, 0.7, 0.05	2.2 < 5°	−0.9	−0.5
14	11	47.0°/0.8, 0.6, 0.0		−0.9	0.7
15	15	47.1°/0.9, 0.5, 0.1	3 < 3.9°	1.0	2.5
16	21b	42.9°/0.8, 0.45, 0.4	2.1 < 3.3°	−3.7	1.1
17	33b	36.0°/0.9, 0.3, 0.3	2.5 < 2.6°	1.3	1.6
18	33c	61.4°/0.7, 0.7, 0.0		−1.7	0.6
19	37b	41.2°/0.9, 0.3, 0.0	2.1 < 2.5°	−0.1	0.6
20	39b	50.7°/0.8, 0.5, 0.3	1.8 < 2.4°	−0.2	0.8
21	*	47.9°/0.7, 0.5, 0.5		−0.5	0.6

[a] Bran. cri. = Brandon's criterion.
* A nearest Σ could not be found.

Ni at different grain boundaries is listed in Table 2. The widths (i.e., full width half maximum, FWHM) of the chromium-concentration profiles lie between 100 and 150 nm. For the sensitized specimens after irradiation to 1 dpa at 450°C, the average Cr concentration at the grain boundaries decreased to about 10.7 at.%, which is 1.7% lower than before irradiation. The widths of the Cr depleted area after irradiation lie between 25 and 50 nm, which are narrower than those before irradiation. From Fig. 2(b), we can also see that when the concentration profiles of Fe, Ni and Si near grain boundaries after irradiation are superposed on those before irradiation, the RIS effect which was occurring in the initially sensitized specimens during irradiation can be seen. Nickel and silicon are enriched at grain boundaries and iron atoms are depleted from the initial Fe-enriched area. The majority of the enriched Ni and Si and the depleted Fe atoms due to the RIS effect at general grain boundaries generally lie in a narrow area with FWHM of 2–4 nm.

3.2. Grain boundary misorientation

In this study, we used Kikuchi patterns to determine the grain boundary misorientation. The details on determining the grain boundary misorientation from Kikuchi lines have been described previously [11]. In general, the measured grain boundaries are not exact CSL boundaries. The deviation from exact CSL, $\Delta\theta$, may be determined by the misorientation matrix [12] and is defined as the average angular difference between the column vectors of the CSL misorientation matrix and the respective column vectors of the measured matrix. The permissible deviation from a CSL can be determined by the Brandon criterion. In this paper, we label a boundary by the nearest Σ, although it may have been over the permissible deviation from a CSL of Σ. The lowest angle/axis pair will be used here to denote the misorientation relationship between the two adjoining grains.

Table 1 summarizes the results of grain boundary misorientation relationships and segregation levels in AR and irradiated 304SS specimens. Some of the grain boundaries for which we cannot find the corresponding nearest Σs for $\Sigma < 43$ are denoted as '*'. In the AR specimens, the enriched Cr atoms were found at grain boundaries and the enrichment level is usually lower on Σ3 boundaries and higher on the unknown boundaries. But, Ni concentration remains at that of the matrix for most of the boundaries. After irradiation to 1 dpa at 450°C, the Cr profiles across grain boundaries were changed. The segregation level in Table 1 indicates that some boundaries, e.g. boundary no. 15 and 17, still show a small amount of Cr enrichment of ΔCr = 1.0, 1.3%,

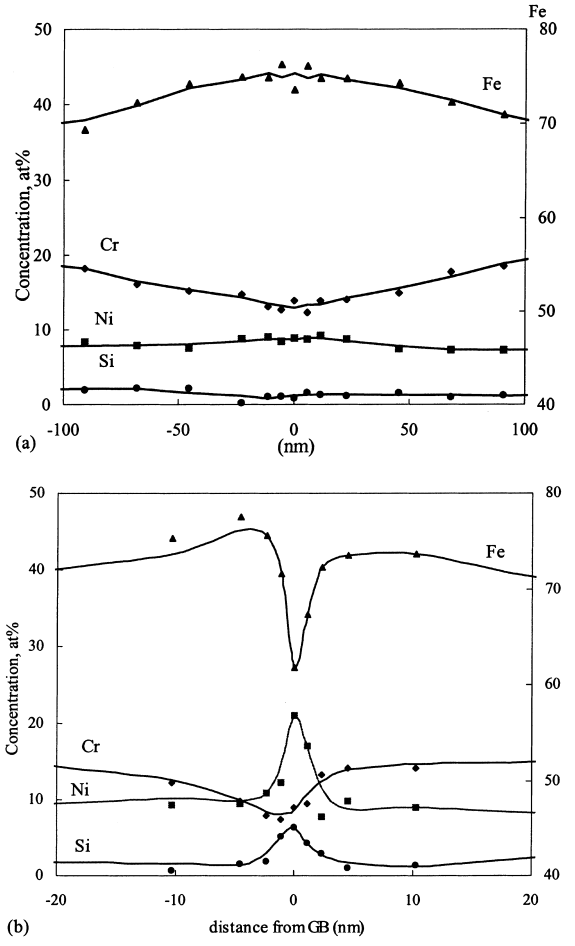

Fig. 2. Concentration profiles near grain boundaries in SEN and SEN + 1 dpa 304SS specimens: (a) Σ27b SEN; (b) Σ27a SEN + 1 dpa.

but others show Cr depletion of $\Delta Cr = -0.1\%$ to -3.7%. This suggests that initially Cr enrichment appears to delay subsequent radiation-induced Cr depletion at grain boundaries, as reported by other workers [13]; and that the delay is different from boundary to boundary, as seen from Table 1.

Table 2 lists the results of grain boundary misorientation relationships and segregation levels of different boundaries in sensitized and irradiated-sensitized 304SS specimens. For sensitized specimens, the variations in Cr segregation level are small (within 10%) for most of the boundaries (not including Σ3 boundary). However, the widths of the Cr-concentration profiles are different from boundary to boundary. The widest Cr-concentration profile in our results was occurring at boundary Σ9 with a FWHM of 151 nm. This result is similar to that of Laws and Goodhew [8] who observed the Σ9 boundary in 316SS with wide Cr-concentration profile and suggested the Σ9 boundary to be a non-favored boundary. For the irradiated sensitized case, the level of Cr depletion looks different from boundary to boundary and the average depletion level after irradiation is deeper than that before irradiation. We noticed from Table 2 that one Σ9 boundary had a slightly smaller amount of Cr depletion than those of other boundaries, and this also infers that Σ9 might have better resistance to radiation sensitization. A similar result has been reported by Avner and Devine [7] who found Σ9 grain boundaries to have a resistance to sensitization in austenitic stainless steels. For Σ9 boundaries, the contradictory results of a wide Cr depleted zones, as found in the above sensitized specimen, and good resistance to sensitization might be reconciled by the high mobility of Σ9 boundary [7].

4. Discussions

In this study, the specimens investigated have different test conditions and results, which are (1) AR with enriched Cr at grain boundaries, (2) AR + 1 dpa with a delay of Cr depletion at boundaries, (3) SEN with Cr depletion at grain boundaries, and (4) SEN + 1 dpa with enriched Ni and deeper and narrower Cr depletion at grain boundaries. From the results of AR + 1 dpa specimens, a delay of Cr depletion at grain boundaries was observed. During irradiation at 450°C, the Cr atoms initially enriched at grain boundaries will diffuse away from the boundary due to the pre-existing concentration gradient and inverse Kirkendall effect. At an earlier time during irradiation, radiation may be thought to enhance the diffusion only; and later on, the RIS effect would dominate after the pre-existing concentration gradient dispersed. In our case it seems that, after irradiation for 1 dpa at 450°C, the pre-existing concentration gradient has dispersed for most of the grain boundaries. We may say that the radiation-induced Cr depletion is occurring with a 1 dpa delay. We can see from Table 1 that the delay is only slightly different from boundary to boundary. It seems that there is no obvious correlation between grain boundary segregation and misorientation in irradiated 304SS specimens with initially enriched Cr at grain boundaries.

From the results of SEN + 1 dpa specimens, we can see that, after irradiation, the Cr-concentration profile changes to narrower and deeper profiles compared to the SEN profiles. During irradiation, the flux equation for solute atom k is given by

$$\Omega J_k = D_k \alpha \nabla C_k + d_{kv} C_k \nabla C_v - d_{ki} C_k \nabla C_i \quad (1)$$

where Ω is the atomic volume, $D_k = d_{kv} C_v + d_{ki} C_i$, d_{kj} = diffusivity of k atom via j defect, C_j = concentration of j, and α = thermodynamic factor. The solute atom flux includes the concentration gradient flux

Table 2
Grain boundary misorientation relationships for SEN and SEN + 1 dpa 304SS specimens

SEN304							
No.	Nearest Σ	Misorientation angle/axis	$\Delta\theta <$ Bran. cri.	ΔCr at.%	ΔNi at.%	FWHM Cr (mm)	FWHM Ni (nm)
1	3	57.8°/0.6, 0.6, 0.6	2.5 < 8.7°	−0.8	0.3	[a]–	–
2	9	41.6°/0.7, 0.7, 0.0	2.4 < 5°	−8.0	1.6	151	–
3	19a	26.5°/0.8, 0.7, 0.1	1.7 < 3.4°	−6.9	1.3	103	–
4	25a	13.7°/1.0, 0.2, 0.1	2.0 < 3°	−6.9	0.6	130	–
5	25a	16.3°/1.0, 0.2, 0.2	2.9 < 3°	−7.7	1.2	124	–
6	27b	32.7°/0.8, 0.6, 0.0		−8.1	1.9	127	–
7	33c	55.3°/0.7, 0.7, 0.1		−7.0	2.1	137	–
SEN + 1 dpa at 450°C							
8	3	59.2°/0.6, 0.5, 0.5	3.7 < 8.7°	−2.7	0.1	–	–
9	3	59.2°/0.6, 0.5, 0.5	3.9 < 8.7°	−1.7	0.6	–	–
10	3	56.5°/0.7, 0.6, 0.5	5.3 < 8.7°	−4.0	−0.2	–	–
11	3	59.8°/0.6, 0.6, 0.5	2.3 < 8.7°	−3.1	0.0	–	–
12	3	59.7°/0.6, 0.6, 0.6	0.4 < 8.7°	−3.6	1.5	–	–
13	3	59.5°/0.6, 0.6, 0.6	1.4 < 8.7°	−1.2	0.6	–	–
14	3	58.4°/0.6, 0.6, 0.5	2.4 < 8.7°	−0.1	−0.1	–	–
15	3	59.7°/0.6, 0.6, 0.6	1.0 < 8.7°	−0.6	−0.5	–	–
16	3	59.9°/0.6, 0.6, 0.5	3.1 < 8.7°	−3.0	0.6	–	–
17	3	59.1°/0.6, 0.6, 0.6	2.2 < 8.7°	−2.8	−0.1	–	–
18	3	59.1°/0.6, 0.6, 0.5	5.0 < 8.7°	−2.9	2.6	10.6	–
19	3	57.5°/0.6, 0.6, 0.5	5.0 < 8.7°	−6.1	5.1	4.8	3.3
20	9	36.3°/0.7, 0.7, 0.1	3.1 < 5.0°	−9.6	2.7	–	–
21	9	36.8°/0.7, 0.7, 0.0	1.9 < 5.0°	−5.7	1.6	–	–
30	11	56.0°/0.7, 0.7, 0.1		−11.9	5.6	35.5	4.6
22	15	48.1°/0.9, 0.5, 0.1	3.5 < 3.9°	−9.5	1.0	–	–
23	15	48.8°/1.4, 0.6, 0.1		−10.2	4.4	28.1	3.3
24	15	44.6°/0.9, 0.4, 0.0	3.4 < 3.9°	−9.4	2.7	49.9	5.2
25	17b	60.4°/0.7, 0.6, 0.4		−10.4	3.7	27.7	3.8
26	21b	46.1°/0.8, 0.5, 0.4	3.1 < 3.3°	−10.5	2.5	–	–
27	21b	41.7°/0.7, 0.5, 0.5		−12.1	7.6	25.1	2.0
28	27a	30.7°/0.8, 0.7, 0.1		−11.3	12.4	28.0	2.3
29	29b	50.5°/0.7, 0.6, 0.4		−10.3	3.2	–	–
31	37c	55.1°/0.7, 0.6, 0.5		−8.9	3.5	31.1	4.1

[a] Not available.

(the first term in Eq. (1)) and the inverse Kirkendall flux (the last two terms in Eq. (1)). In the specimens with a pre-existing Cr depletion profile due to thermal sensitization, the concentration gradient flux will compete with the inverse Kirkendall flux during irradiation. If the inverse Kirkendall flux is greater than the concentration gradient flux near grain boundaries, Cr will be further depleted at grain boundaries after irradiation. In a region away from grain boundary, where the concentration gradient flux exceeds the inverse Kirkendall flux, Cr will increase in that region, and hence provide a narrow profile. Similar results were reported by Okada [14] who investigated the effects of thermal sensitization on RIS in 304SS irradiated with He ions.

In the CSL model, CSL boundaries generally have an energy of a local minimum. As can be seen from energy-misorientation curves, normally there are cusps occurring at CSL boundaries. In the case of grain boundary segregation, we believe that the cusps should be occurring at CSL boundaries also. Fig. 3 displays the measured variation of Cr segregation level with the misorientation angle, θ, with rotation axis $\langle 2\,1\,0\rangle$ in the radiated sensitized specimens. We can see that three cusps appear at $\Sigma 3$, $\Sigma 9$ and $\Sigma 15$ boundaries in Fig. 3. In order to obtain the cusps by data fitting, we assume that the shape of the segregation cusp is similar to that of the boundary energy cusp. Therefore, the segregation cusp may be written as,

$$S = S_{\mathrm{CSL}} + A(\theta - \theta_{\mathrm{CSL}})(B - \ln(\theta - \theta_{\mathrm{CSL}})), \tag{2}$$

where S is the segregation level (defined as concentration at grain boundary minus that in the matrix.), S_{CSL} is segregation level at a CSL boundary, θ is misorientation angle between the two adjoining grains, and A and B are parameters related to elastic constants and dislocation

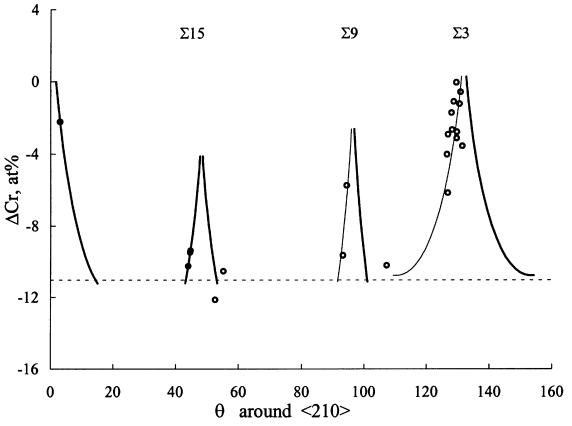

Fig. 3. The variations of Cr segregation level with misorientation angle, θ, with rotation axis $\langle 2\,1\,0\rangle$, in radiated sensitized 304SS specimens. Three cusps appear at $\Sigma 3$, $\Sigma 9$ and $\Sigma 15$.

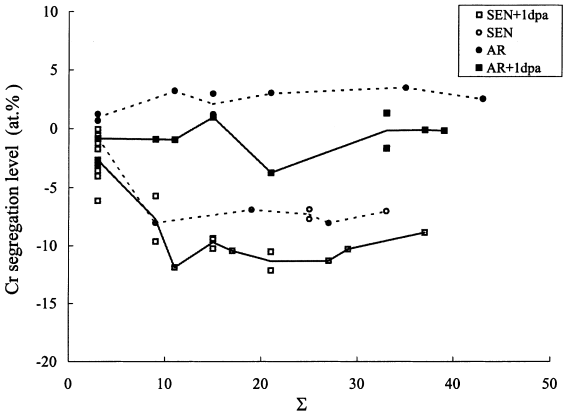

Fig. 4. Variations of Cr segregation level with Σ for AR, SEN, AR + 1 dpa, and SEN + 1 dpa 304SS specimens.

cores, respectively. Actually, Eq. (2) can be derived from the Gibbs adsorption equation, $[\partial\sigma/\partial\mu_2]_{T,P} = -\Delta N_2$, where σ is the interface free energy, μ_2 the chemical potential of solute 2, and ΔN_2 the 'interface excess' of solute 2. In curve fitting, we fit Eq. (2) to the measured points by the method of least squares. We can see from the fitted cusps that the Cr segregation level at special boundaries in the irradiated sensitized specimens seems to increase with Σ for values up to $\Sigma = 15$. In this study, the cusps were found to occur at $\Sigma 3$ boundaries in all the specimens and at $\Sigma 9$ and $\Sigma 15$ in the irradiated sensitized specimens. As for the other boundaries, the data obtained here are insufficient to see a clear cusp, if there is any. For boundaries other than $\Sigma 3$, $\Sigma 9$ and $\Sigma 15$, random or near CSL, variations in Cr segregation level are small in specimens of each type, as can be seen from Fig. 4 which shows the variations of segregation level with Σ for AR, SEN and their irradiated specimens.

5. Summary

The effects of grain boundary misorientation on grain boundary segregation were investigated for specimens of AR, irradiated, sensitized and irradiated sensitized 304SS. The main results are summarized as follows:

1. For the AR specimens with enriched Cr at grain boundaries, a delay compared to no pre-enrichment of Cr depletion at grain boundaries was observed after 1 dpa irradiation at 450°C. The conventional RIS effect would dominate after the pre-existing concentration gradient dispersed.
2. For the sensitized specimens after 1 dpa irradiation at 450°C, the Cr-concentration profile gets narrower and deeper than that of the SEN profile. During irradiation, the solute atom flux will include both the concentration gradient flux and the inverse Kirkendall flux, and these two fluxes will compete with each other. Cr will be further depleted at grain boundaries if the inverse Kirkendall flux is greater than the concentration gradient flux. The Cr profile would be more narrower if the concentration gradient flux is dominant on both sides of the grain boundary.
3. Segregation cusps were found at the $\Sigma 3$ grain boundary in all of the specimens investigated. Therefore, the $\Sigma 3$ boundary is a very special boundary which has good resistance to solute segregation for all of the specimens of AR, SEN and irradiated types.
4. From the fitted segregation cusps, it seems that the Cr segregation level at special boundaries in irradiated sensitized 304 stainless steels increase with Σ for values up to $\Sigma = 15$.

Acknowledgements

This study was supported by Center of Electron Microscopy for FEGTEM/EDS observation and Van de Graaff Accelerator Center for proton irradiation in National Tsing Hua University. This work was financially supported by the National Science Council of the Republic of China, Taiwan under contract number of NSC-88-2212-E-007-41.

References

[1] A. Otsuki, M. Mizuno, in: Proceedings of JIMIS-4, Transactions of Japan Institute of Metals (Suppl.) 27 (1986) p. 789.
[2] K.T. Aust, J.W. Rutter, Trans. AIME 215 (1959) 119.
[3] W. Lange, M. Jurisch, Grain Boundary Structure and Kinetics, in: H. Mykura (Eds.), American Society for Metals, Metals Park, OH, 1980 p. 209.
[4] T. Watanabe, J. de Physique, 46, Colloue C4, suppl. au no. 4, 1985, c4–555.

[5] C.L. Briant, Acta Metall. 31 (1983) 257.
[6] D.G. Brandon, Acta Metall. 14 (1966) 1479.
[7] T.M. Devine, J. Mater. Sci. 32 (1997) 1555.
[8] M.S. Laws, P.J. Goodhew, Acta Metall. Mater. 39 (1991) 1525.
[9] G.S. Was, P. Andresen, J. Metals 44 (4) (1992) 8.
[10] H. Wiedersich, P.R. Okamoto, Interfacial Segregation, in: W.C. Johnson, J.M. Blakely (Eds.), American Society for Metals, Metals Park, OH, 1979, p. 450.
[11] T.S. Duh, J.J. Kai, F.R. Chen, L.H. Wang, J. Nucl. Mater. 258–263 (1998) 2064.
[12] V. Randle, B. Ralph, J. Mater. Sci. 21 (1986) 3823.
[13] E.P. Simonen, S.M. Bruemmer, in: Proceedings of the Eighth International Symposium on Environmental Degradation of Materials in Nuclear Power System–Water Reactors, vol. 2, 1997, p. 751.
[14] O. Okada, K. Nakata, S. Kasahara, J. Nucl. Mater. 265 (1999) 232.